Translational Oncology
www.transonc.com

Volume 11 Number 4 August 2018 pp. 962–970 962

Molecular Characterization and Putative Pathogenic Pathways of Tuberous Sclerosis Complex–Associated Renal Cell Carcinoma

Jeong Hwan Park[*,†], Cheol Lee[*], Mee Soo Chang[*,†], Kwangsoo Kim[‡], Seongmin Choi[‡], Hyunjung Lee[§], Hyun-Seob Lee[§] and Kyung Chul Moon[*,¶]

[*]Department of Pathology, Seoul National University College of Medicine, Seoul, Republic of Korea; [†]Department of Pathology, SMG-SNU Boramae Medical Center, Seoul, Republic of Korea; [‡]Division of Clinical Bioinformatics, Biomedical Research Institute, Seoul National University Hospital, Seoul, Republic of Korea; [§]Genomic Core Facility, Department of Transdisciplinary Research and Collaboration, Biomedical Research Institute, Seoul National University Hospital, Seoul, Republic of Korea; [¶]Kidney Research Institute, Medical Research Center, Seoul National University College of Medicine, Seoul, Republic of Korea

Abstract

Tuberous sclerosis complex–associated renal cell carcinoma (TSC-RCC) has distinct clinical and histopathologic features and is considered a specific subtype of RCC. The genetic alterations of *TSC1* or *TSC2* are responsible for the development of TSC. In this study, we assessed the mTOR pathway activation and aimed to evaluate molecular characteristics and pathogenic pathways of TSC-RCC. Two cases of TSC-RCC, one from a 31-year-old female and the other from an 8-year-old male, were assessed. The mTOR pathway activation was determined by immunohistochemistry. The mutational spectrum of both TSC-RCCs was evaluated by whole exome sequencing (WES), and pathogenic pathways were analyzed. Differentially expressed genes were analyzed by NanoString Technologies nCounter platform. The mTOR pathway activation and the germline mutations of *TSC2* were identified in both TSC-RCC cases. The WES revealed several cancer gene alterations. In Case 1, genetic alterations of *CHD8*, *CRISPLD1*, *EPB41L4A*, *GNA11*, *NOTCH3*, *PBRM1*, *PTPRU*, *RGS12*, *SETBP1*, *SMARCA4*, *STMN1*, and *ZNRF3* were identified. In Case 2, genetic alterations of *IWS1* and *TSC2* were identified. Further, putative pathogenic pathways included chromatin remodeling, G protein–coupled receptor, Notch signaling, Wnt/β-catenin, PP2A and the microtubule dynamics pathway in Case 1, and mRNA processing and the PI3K/AKT/mTOR pathway in Case 2. Additionally, the *ALK* and *CRLF2* mRNA expression was upregulated and *CDH1*, *MAP3K1*, *RUNX1*, *SETBP1*, and *TSC1* mRNA expression was downregulated in both TSC-RCCs. We present mTOR pathway activation and molecular characteristics with pathogenic pathways in TSC-RCCs, which will advance our understanding of the pathogenesis of TSC-RCC.

Translational Oncology (2018) 11, 962–970

Introduction

Renal cell carcinoma (RCC) is one of the most fatal genitourinary tumors and accounts for approximately 90% of renal cancers [1]. Histopathologic features and molecular studies have identified and classified various subtypes of RCC [2, 3]. These subtypes include clear cell RCC (CCRCC), papillary RCC (PRCC), chromophobe RCC (ChRCC), MiT family translocation RCC, and clear cell papillary RCC. Additionally, syndrome-associated hereditary renal cell tumors, including Von Hippel–Lindau syndrome, hereditary papillary RCC,

Address all correspondence to: Kyung Chul Moon, MD, PhD, Department of Pathology and Kidney Research Institute, Medical Research Center, Seoul National University College of Medicine, 103 Daehak-ro Jongno-gu, Seoul, 03080, Korea.
E-mail: blue7270@snu.ac.kr
Received 12 April 2018; Revised 24 May 2018; Accepted 24 May 2018

1936-5233/18
https://doi.org/10.1016/j.tranon.2018.05.010

and tuberous sclerosis, have been identified. The National Cancer Data Base revealed 5-year survival rates of 80.9% in stage I, 73.7% in stage II, 53.3% in stage III and 8.2% in stage IV kidney cancer patients [4]. Various aspects of the treatment for advanced RCC and metastatic RCC have been studied, and target therapy and immunotherapy have showed considerable improvement in patient survival [5–7].

Tuberous sclerosis complex–associated RCC (TSC-RCC) is an emerging subtype of RCC [8, 9]. TSC showed autosomal dominant inheritance and was characterized by multisystem disorders, including epilepsy, developmental delay, angiofibromas, hypomelanotic macules, cortical dysplasias, lymphangioleiomyomatosis, and angiomyolipoma (AML) [10, 11]. The disease is caused by alterations in *TSC1* or *TSC2* genes, which encode hamartin and tuberin, respectively [10]. Studies of TSC-RCC from multiple institutions have revealed the clinical and histopathologic features of TSC-RCC [8, 9]. Clinically, TSC-RCC is characterized by an association with TSC, female predominance, early age of onset, and indolent clinical outcomes. Histopathologically, TSC-RCC has been classified according to several distinct morphologies, including renal angiomyoadenomatous tumor (RAT)–like, TSC-associated papillary RCC, chromophobe-like or hybrid oncocytic/chromophobe tumor (HOCT)–like, eosinophilic/macrocystic, and unclassified RCC.

Cancer genomics have greatly expanded our knowledge of cancer biology. In kidney cancers, CCRCC, PRCC, and ChRCC were analyzed, and important genomic events and pathways were elucidated [12–14]. Moreover, actionable targets for RCC have been identified, and patients with those alterations have been enrolled in clinical trials [15, 16]. As precision medicine has been initiated in earnest, unveiling the genomic landscape of cancer has progressed, resulting in promising improvements in treatment modalities and patient prognoses [17, 18]. Additionally, studies of rare but specific genetic alterations, such as those in TSC-RCC, will advance our understanding of cancer biology and the discovery of novel cancer-related genes.

In this study, we assessed the activation of the mTOR pathway and the genetic alterations in two cases of TSC-RCC by immunohistochemistry and whole exome sequencing (WES). Additionally, we analyzed mRNA expression of cancer genes. We aimed to evaluate the mutation spectrum of both patients and search for the genetic basis of the pathogenesis and actionable targets of TSC-RCC.

Material and Methods

Patient Selection and Clinicopathologic Review

We retrospectively reviewed all RCCs surgically removed by radical or partial nephrectomy between January 1, 2009, and December 31, 2014, at Seoul National University Hospital. We reviewed the medical records to identify TSC patients and identified two cases of TSC-RCC. Each TSC-RCC was evaluated with regard to the clinical and histopathologic features, such as history of epilepsy, RCC histologic type, WHO/ISUP grade [19], and the stage of the tumor [4]. Disease progression was determined based on the clinical and radiographic findings and the patients' medical records. This study was approved by the Institutional Review Board of Seoul National University Hospital (IRB No. H-1602-040-739).

Immunohistochemistry

We performed immunohistochemistry on a representative slide from TSC-RCC cases (Supplementary Table 1). For the differential diagnosis, we assessed pan-cytokeratin, HMB-45, Melan A, CD10, CK7, and c-kit immunoreactivity. To evaluate mTOR pathway activation, we assessed phospho-mTOR immunoreactivity. Immunohistochemical staining was performed using autostainers for each antibody. The binding of the primary antibody was detected using a detection kit according to the manufacturer's instructions.

WES and Bioinformatics Analysis [12–14, 20–37]

Normal and cancer tissue were obtained from formalin-fixed, paraffin-embedded tissue block in both TSC-RCCs. DNA was extracted, and the quality of DNA was checked. WES was performed using HiSeq 2500 sequencing system (Illumina). Sequencing libraries were prepared, and adapter ligated DNA was amplified. Sequence was mapped to NCBI b37 human reference genome sequence, and BAM files were realigned. Germline and somatic mutation calling was performed. The alterations of cancer-related genes were identified. Detailed methods are described in Supplementary methods (Supplementary Figure 1, Supplementary Tables 2 and 3).

Copy Number Variation and Loss of Heterozygosity Analysis [22, 38–41]

Copy number variations (CNVs) and large loss of heterozygosities (LOHs) were assessed in WES data. In each case, read count was evaluated and normalized using paired normal and cancer sequencing data. The reads per kilobase million (read count/exon length/total read count $\times 10^9$) ratio was assessed for detecting amplification or deletion. VAF was evaluated for assessing the CNVs in megabase scale. Detailed methods are described in Supplementary methods.

Validation of Cancer Genes Alterations

We performed Sanger sequencing for the validation of cancer genes in TSC-RCC cases. Additionally, we performed droplet digital PCR for cancer genes in TSC-RCC Case 1 due to low tumor purity (inflammatory cell infiltration) and obscuring factors (abscess). Detailed methods are described in supplementary methods (Supplementary Tables 4 and 5).

Pathway Analysis

For the analysis of pathogenic pathways for each TSC-RCC, we selected cancer genes according to the following criteria: depth (≥10×), VAF (≥20%), score (≥3), no strand bias, altered function (≥1 prediction method), tumor suppressor genes (TSGs), or oncogenes (OGs) [31]. We used KEGG pathway maps (http://www.genome.jp/kegg/pathway.html) [36, 37] and Ingenuity pathway analysis (http://www.ingenuity.com/products/ipa) [42] for pathway analysis. Additionally, we used STRING (http://string-db.org) [43] for assessment of protein-protein interaction networks.

mRNA Expression Analysis

Total RNA was extracted using an eCube RNA Mini Kit (Philekorea Technology, Seoul, Korea). RNA yield and purity were assessed using a DS 11 Spectrophotometer (Denovix Inc., DE, USA). Total RNA (300 ng) was added to the sample preparation reaction in the available 5 μl volume. RNA quality was verified using a Fragment Analyzer (Advanced Analytical Technologies, IA, USA). The digital multiplexed nanoString nCounter human mRNA expression assay (nanoString Technologies) was performed. The mRNA data analysis was performed using the nSolver software analysis. The mRNA profiling data were normalized using housekeeping genes.

Comparison with Reported Data and Public Database

We analyzed the sequencing results with the COSMIC, TCGA, and cBioPortal database [12, 13, 33–35]. Genetic alterations were compared

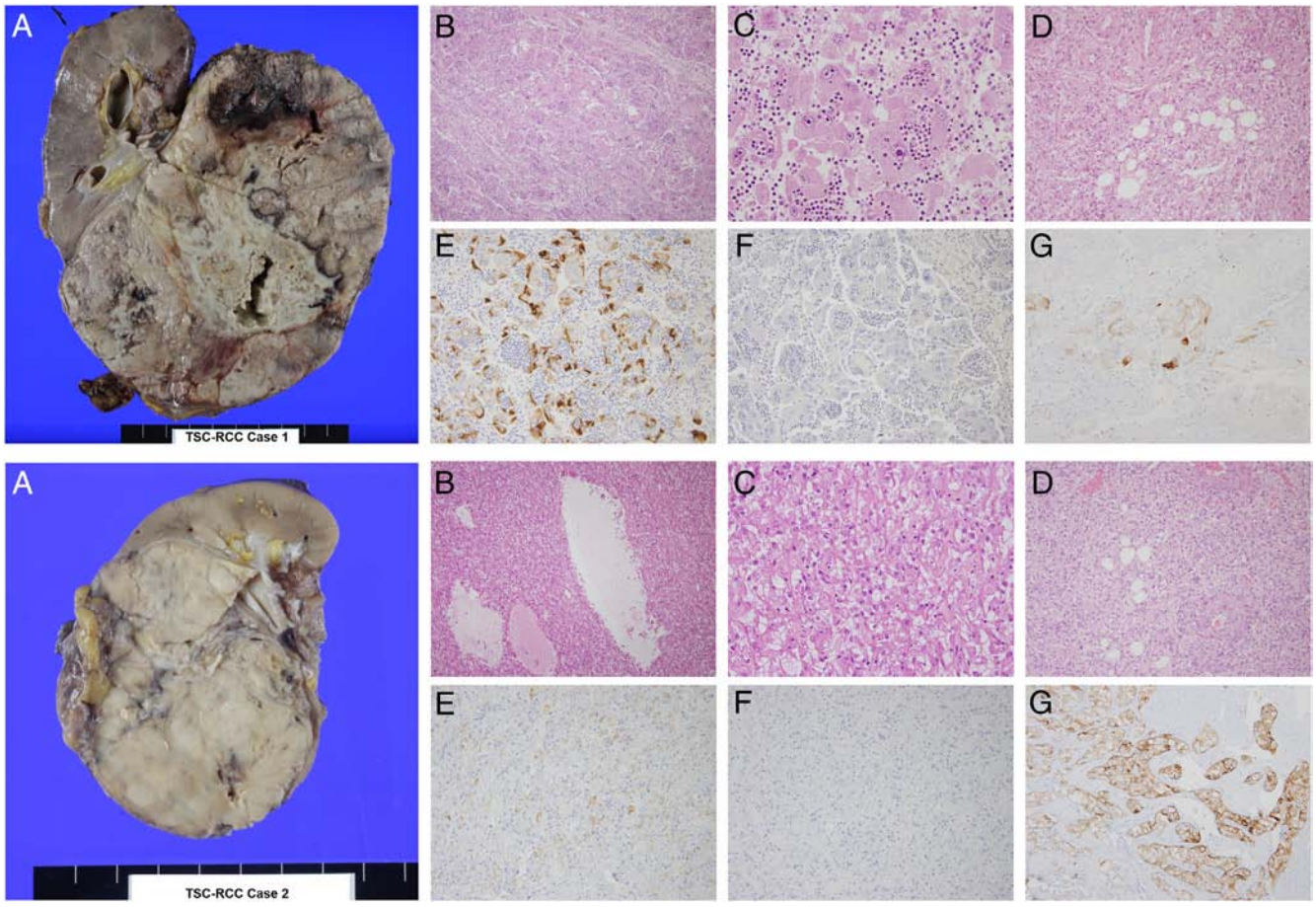

Figure 1. Pathologic features of TSC-RCC Case 1 (upper panel) and Case 2 (lower panel). (A) Macroscopic findings. (B-D) Histopathologic findings [(B) low-power view, (C) high-power view, (D) angiomyolipoma] and (E-G) Immunohistochemical findings [(E) pan-cytokeratin, (F) HMB-45, (G) phospho-mTOR]. Original magnification ×100 (B), ×200 (D-G), and ×400 (C).

to common RCCs (CCRCC, PRCC, and ChRCC) sequencing data [12–14]. Also, we compared our results to genetic data of TSC-associated papillary RCC [44] and molecular characteristics of eosinophilic/macrocystic RCC [45, 46]. Potential actionable targets were evaluated by matching molecular targets of FDA-approved drugs [47] and Tumor Alterations Relevant for GEnomics-driven Therapy database (http://www.broadinstitute.org/cancer/cga/target).

Results

Clinical Features of TSC-RCC Patients

The Case 1 patient was a 31-year-old female with a history of seizures from a young age who was clinically diagnosed with TSC for her facial angiofibromas and subependymal nodules. The patient had multiple renal masses, and one of them was diagnosed as AML. Upon follow-up, she visited the hospital for abdominal pain, and a 15.4 × 10.0–cm mass was detected in the right kidney. The Case 2 patient was an 8-year-old male with a history of seizures from 12 months who was suspected to have TSC due to his facial angiofibromas. On workup, multiple subependymal nodules and cortical tubers were identified. Additionally, a 5.2 × 7.1 × 6.0–cm mass was detected in the left kidney. Radical nephrectomy was performed on both patients.

Histopathologic Features of TSC-RCC Cases

The TSC-RCC Case 1 consisted of a 16.5 × 10.5 × 7.9–cm solid mass with hemorrhage and necrosis (Figure 1, upper panel). The tumor showed sheet-like growth pattern and was composed of discohesive large atypical cells with ample, light eosinophilic cytoplasm and vesicular nucleus with prominent nucleolus. The emperipolesis, neutrophilic infiltration, and abscess as well as angiolymphatic invasion were identified. WHO/ISUP grade was 4 and pTNM stage was II (pT2bN0M0). The TSC-RCC Case 2 consisted of a 7.3 × 5.3 × 4.0–cm solid mass with focal cystic change (Figure 1, lower panel). The tumor showed trabecular growth with atypical cells with plump, eosinophilic, and granular cytoplasm. The tumor cells revealed vesicular and wrinkled nuclei with small nucleoli. The cysts showed hobnail pattern of cyst lining cells with plump eosinophilic granular cytoplasm. Additionally, the tumor revealed hyalinized stroma. The angiolymphatic invasion was identified. WHO/ISUP grade was 2 and pTNM stage was II (pT2aN0M0). Both cases had multiple renal AMLs. The Case 2 patient had multiple variable-sized renal cysts lined by epithelial cells with plump eosinophilic cytoplasm, which was reported as a histologic feature of epithelial cysts in TSC [48] or cuboidal cells. Immunohistochemically, both cases were negative for myomelanocytic markers (HMB-45, Melan A) and positive for epithelial marker (pan-cytokeratin), suggesting RCC rather than epithelioid AML. Case 1 can be classified as unclassified RCC and Case 2 as RCC with eosinophilic/macrocystic feature. Additionally, phospho-mTOR was positive in TSC-RCCs but not in adjacent unaffected renal parenchyma.

Germline Mutations of TSC1 or TSC2 Genes in TSC-RCC Cases

We regarded identical mutations on both normal and cancer tissues as germline mutations. In Case 1, a *TSC2* c.4707C > A (p.Tyr1569*) mutation was identified, and in Case 2, a *TSC2* c.2548+2 T > G mutation was seen (Table 1 and Supplementary Figure 2), which were stop gained effect and a splice donor variant, respectively.

Somatic Mutations and Alterations of Cancer-Related Genes in TSC-RCC Cases

The somatic mutations of SNV or small indels were analyzed (Supplementary Figure 3, Supplementary Tables 6 and 7). In Case 1, a total of 589 mutations (567 SNVs, 1 insertion, and 21 deletions) were identified. In Case 2, a total of 258 mutations (257 SNVs and 1 deletions) were identified. Further, alterations of cancer-related genes were assessed. In Case 1, 72 cancer-related genes were identified (Figure 2A and Supplementary Table 8). There were 69 SNVs and 3 deletions, including 58 missense mutations, 6 nonsense mutations, 5 splice site SNVs, 2 in frame deletions and 1 frame shift deletion. In Case 2, we identified 32 altered cancer-related genes (Figure 2B and Supplementary Table 9). There were 31 SNVs and 1 deletion, including 23 missense mutations, 5 nonsense mutations, 3 splice site SNVs, and 1 frame shift deletion.

Genetic Alterations of Cancer Genes in TSC-RCC Cases

To assess the pathogenic basis of each TSC-RCC case, we analyzed alterations of cancer genes (Table 2). In Case 1, 12 cancer genes were identified. These included *CHD8*, *CRISPLD1*, *EPB41L4A*, *GNA11*, *NOTCH3*, *PBRM1*, *PTPRU*, *RGS12*, *SETBP1*, *SMARCA4*, *STMN1*, and *ZNRF3*. All mutations were classified as SNVs, and there were 9 missense mutations, 1 nonsense mutation, and 2 splice site SNVs. In Case 2, we identified 2 altered cancer genes. These included *IWS1* and *TSC2*. All mutations were classified as SNVs, and there were 1 nonsense mutation and 1 splice site SNVs. Above genes were validated by droplet digital PCR and Sanger sequencing (Supplementary Figure 4).

CNV and Loss of Heterozygosity in TSC-RCC Cases

In both TSC-RCCs, there were no megabase-scale amplification or deletion. Also, LOH including chromosome 16 (*TSC2*, chr.16p13.3) was not found in both TSC-RCCs (Supplementary Figures 5 and 6).

Putative Pathogenic Pathways in TSC-RCC Cases

We assess putative pathogenic pathways for each TSC-RCC case (Figure 3 and Table 3). In Case 1, putative pathogenic pathways were chromatin remodeling pathway (*CHD8*, *PBRM1* and *SMARCA4*), G protein–coupled receptor (GPCR) pathway (*GNA11* and *RGS12*), Notch signaling pathway (*NOTCH3*), Wnt/β-catenin pathway (*PTPRU* and *ZNRF3*), PP2A pathway (*SETBP1*), and microtubule dynamics pathway (*STMN1*). In Case 2, putative pathogenic pathways were mRNA processing (*IWS1*) and PI3K/AKT/mTOR pathway (*TSC2*).

Genetic Alterations in RCC-Related Genes

Several RCC-related gene alterations were identified (Supplementary Figure 7 and Supplementary Table 10). In Case 1, these included *AHNAK2* (CCRCC), *CUBN* and *SMARCA4* (PRCC), *AFF3*, *CDC27*, *DSPP*, *PRODH*, *TTN*, *YLPM1* and *ZNF598* (ChRCC), *KMT2C* and *PBRM1* (CCRCC and PRCC), and *MUC2* (CCRCC, PRCC and ChRCC). Additionally, *FH*, *KMT2C* and *PBRM1* genes were in common with unclassified RCC. In Case 2, only *TG* (ChRCC) was identified. Additionally, the *TSC2* gene was in common with unclassified RCC. The *USP34* (Case 1) and *NDE1* (Case 2) alterations in TSC-associated papillary RCC were found.

Potential Actionable Targets in TSC-RCC Cases

In Case 1, we identified three potentially actionable targets. These included *GNA11*, *NOTCH3*, and *ZNRF3* for which MAPK pathway inhibitors, gamma secretase inhibitors, and porcupine inhibitors can be considered, respectively. In Case 2, there was one potentially actionable target. It was *TSC2,* and mTOR inhibitors can be considered for targeted therapy.

Differentially Expressed Genes in TSC-RCC Cases

We assessed 770 genes to identify differentially expressed genes (DEGs) (Supplementary Table 11). Case 1 includes 20 upregulated and 33 downregulated genes with a two-fold change, and Case 2 has 202 upregulated and 308 downregulated genes with a two-fold change (Supplementary Table 12). Among those, the *ALK* and *CRLF2* mRNA expression was upregulated and *CDH1*, *MAP3K1*, *RUNX1*, *SETBP1*, and *TSC1* mRNA expression was downregulated in both TSC-RCCs. Cancer-related pathways with DEGs are presented in Supplementary Figures 8 and 9.

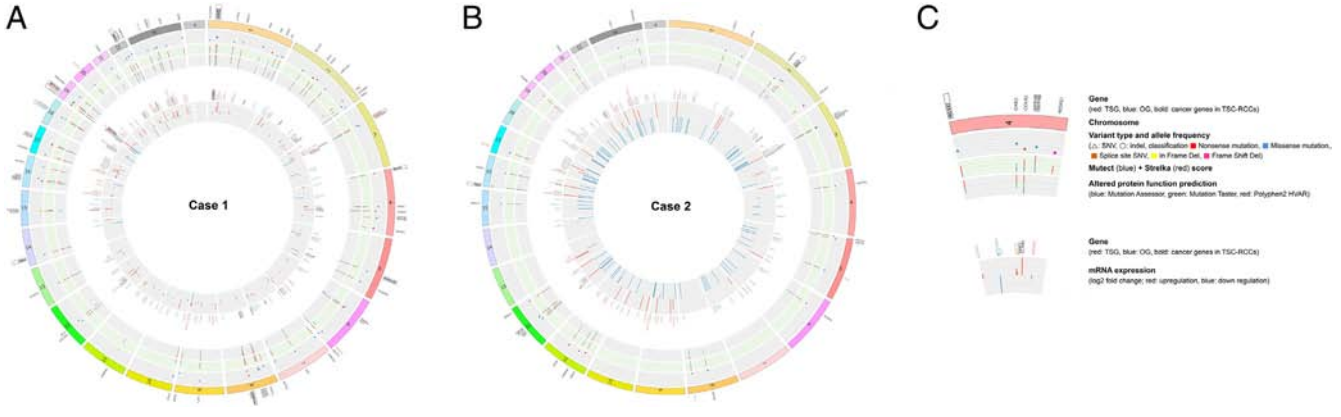

Figure 2. Somatic mutational spectrum of cancer-related genes in TSC-RCC cases. (A) TSC-RCC Case 1 and (B) TSC-RCC Case 2. (C) Circos plot inset legend.

Table 1. Germline Mutations of *TSC1* or *TSC2* Genes in Two Cases of TSC-RCC

Case	Gene	rsID	Reference	Alternate	Variant Type	Effect	Impact	Feature Type	HGVS.c	HGVS.p	1000G Maf	1000G ASN Maf	VAF (%)	Polyphen2 HVAR	SIFT	Validation*
1	*TSC2*	.	C	A	SNV	Stop gained	HIGH	Transcript	c.4707C > A	p.Tyr1569*	NA	NA	45.35	.	.	+
2	*TSC2*	.	T	G	SNV	Splice donor variant	HIGH	Transcript	c.2578+ 2 T > G	.	NA	NA	52.00	.	.	+

Abbreviations: *NA*, not available; *VAF*, variant allele frequency.

* Sanger sequencing and droplet digital PCR were performed in normal and tumor tissues from both cases.

Discussion

The histopathologic features of TSC-RCC have been elucidated [8, 9]. One study classified them as TSC-associated papillary RCC (52%, 24 cases), HOCT (33%, 15 cases), and unclassified RCC (15%, 7 cases) [9]. The authors emphasized the uniformly deficient expression of SDHB in TSC-associated papillary RCC. Another study classified TSC-RCC as RAT-like (30%, 17 cases), chromophobe-like (59%, 34 cases), and eosinophilic/macrocystic RCC (11%, 6 cases) [8]. Though those studies classified different histopathologic subtypes, TSC-associated papillary RCC and RAT-like RCC have similar

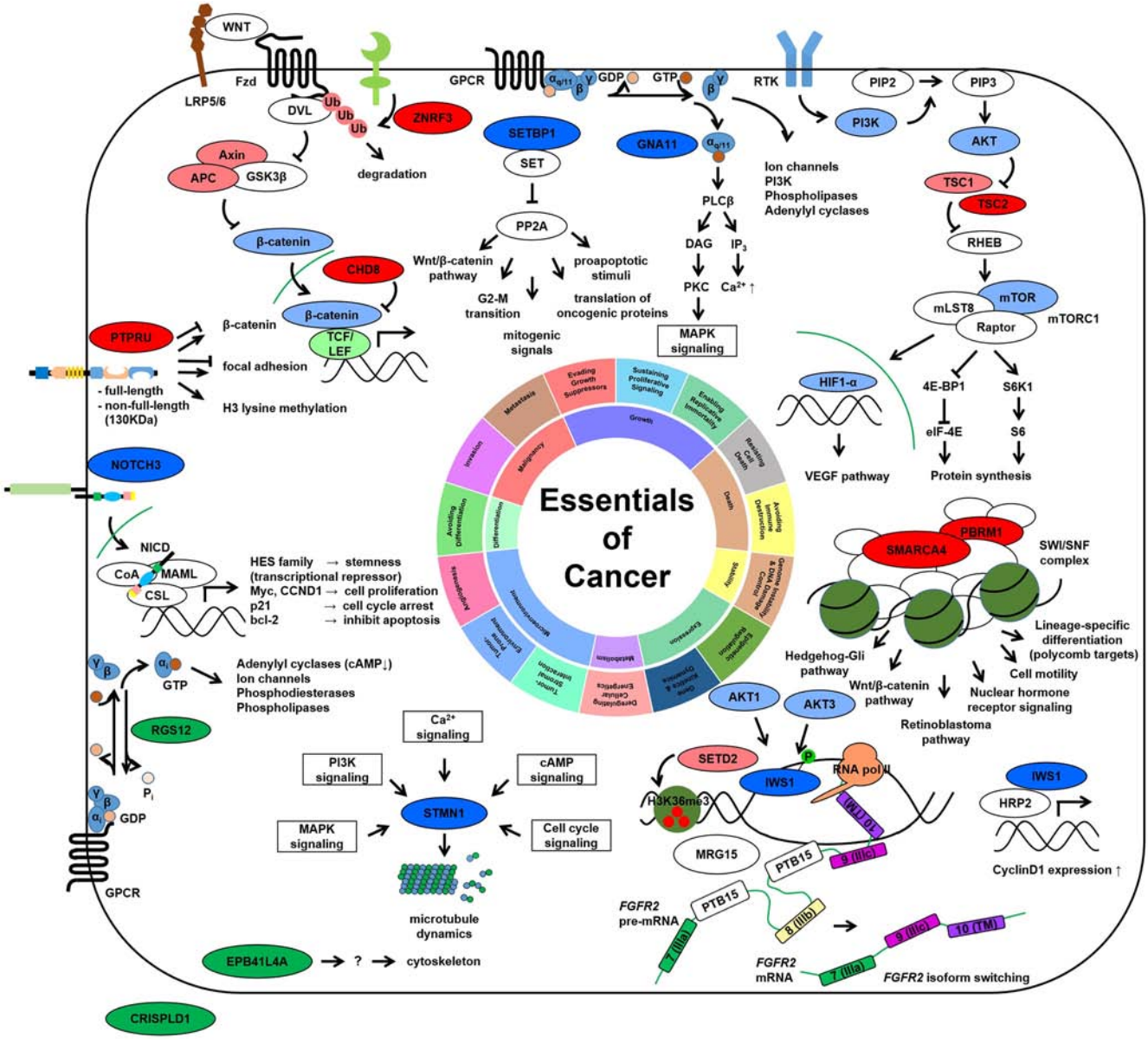

Figure 3. Putative pathogenic pathways in TSC-RCC cases (red: tumor suppressor gene; blue: oncogene; bold: cancer genes in TSC-RCCs).

histologic features and could be categorized as RCC with (angio) leiomyomatous stroma [3]. Also, HOCT and chromophobe-like RCC could be regarded as one subtype.

The mTOR activation has been thought to be one of the pathogenic alterations in TSC-RCC because alterations of *TSC1* or *TSC2* genes were responsible for the development of TSC. However, the pathogenic role of mTOR activation on TSC-RCC pathogenesis has not been studied. We identified mTOR activation by phospho-mTOR immunohistochemistry. Our results suggest that the mTOR pathway is activated and responsible for the pathogenesis and serves as a rationale for the possible use of mTOR inhibitor in our two patients with TSC-RCC.

We performed WES and reported genetic alterations in TSC-RCC, especially first results of unclassified and eosinophilic/macrocystic RCC. There were genetic analysis of 5 TSC-associated papillary RCC cases from 1 patient and molecular karyotyping of 15 eosinophilic/macrocystic RCC cases without clinical evidence of TSC [44–46]. In TSC-associated papillary RCC cases, there were second-hit mutations (3 SNVs, 1 indel, and 1 LOH) in *TSC2*, and somatic mutations of *PROS1*, *NPFFR2*, *TLL2*, and *RASA1* were identified [44]. In sporadic cases of eosinophilic/macrocystic RCC, copy number gain of 16p-q, 7p-q, 13q, 19p, 1p, and 10q; copy number loss of Xp, 22q, 19p,19q, and Xq; and LOH in 16p, Xq, 11p, and 9q were identified [45, 46].

In our cases, the germline mutations of *TSC2* were identified, a *TSC2* nonsense mutation in Case 1 and a *TSC2* splice donor variant mutation in Case 2. For the development of tumors related to TSC, biallelic *TSC2* inactivation is needed. However, we could not find additional *TSC2* mutations or LOH in Case 1. There is the possibility that other types of mutations (large indel or epigenetic alterations), not detected in WES, may exist in the Case 1 patient or *TSC2* inactivation was not responsible for mTOR activation, and tumor progression as histopathologic feature of Case 1 was truly unclassifiable. In Case 2, there was additional *TSC2* somatic mutation.

The somatic mutation analysis showed different genetic mutation profiles from common RCCs. In Case 1, all genetic alterations, except *KMT2C* (in PRCC) and *PBRM1* (in CCRCC), were found with a less than 5% frequency with those in common RCCs. In Case 2, there were no common genes, except the *TG* gene, which showed 3.08% frequency with those in ChRCC. These genetic features support the idea that TSC-RCC should be classified as a distinct entity. The *USP34* and *NDE1* alteration in TSC-associated papillary RCC was found in Case 1 and 2, respectively.

We aimed to elucidate the pathogenic basis of TSC-RCC. In Case 1, we selected 12 cancer genes and identified 6 pathways. The *CHD8* gene acts as a TSG and is associated with the chromatin remodeling pathway and affects cell survival and cell proliferation. *CHD8* c.2368C > T, p.R790C mutation was previously reported in malignant melanoma and is considered pathogenic based upon FATHMM [33]. The pathogenic role on cancer of *CRISPLD1* and *EPB41L4A* genes was not studied well. *CRISPLD1* c.1363C > T, p.R455* was in LCCL domain and has not been previously reported. Also, *EPB41L4A* c.1618C > T, p.R540C mutation has not been previously reported. The *GNA11* gene is an OG and is a component of GPCR pathway and involved in cell proliferation, invasion, and differentiation. *GNA11* c.604C > T, p.R202W mutation located in G-alpha domain has not been previously reported. The *NOTCH3* gene acts as OG and belongs to Notch signaling pathway and is involved in stem-like properties, cell differentiation, and proliferation. *NOTCH3* c.1194C > T, p.G398G mutation in EGF_CA domain has previously been reported in urothelial

Table 2. Somatic Mutations of Cancer Genes in TSC-RCC Patients

Case	Score	Gene	Driver	Role	Variant Classification	Variant Type	Reference	Alternate	dbSNP RS	cDNA Change	Protein Change	Mutation Assessor	Mutation Taster	Polyphen2 HVAR	Mutect	Strelka	VAF (%)	Validation
1	3	*CHD8*	.	.	Missense mutation	SNV	G	A	.	c.2368C > T	p.R790C	M	D	D	1	2	22.22	+[a]
	3	*CRISPLD1*	.	.	Nonsense mutation	SNV	C	T	rs149361480	c.1363C > T	p.R455*	.	A	.	1	2	36.36	NA
	3	*EPB41L4A*	.	.	Missense mutation	SNV	G	A		c.1618C > T	p.R540C	M	D	D	1	2	28.57	NA
	3	*GNA11*	+	OG	Splice site	SNV	C	T	.	c.604C > T	p.R202W	H	D	D	1	2	28.57	+[a]
	4	*NOTCH3*	.	.	Splice site	SNV	G	A	rs140368657	c.1194C > T	p.G398G	.	.	.	2	2	25	+[a]
	3	*PBRM1*	+	TSG	Missense mutation	SNV	C	T	.	c.49G > A	p.G17R	L	D	D	1	2	21.05	+[a]
	4	*PTPRU*	.	.	Missense mutation	SNV	G	A	rs35745442	c.1412G > A	p.R471H	M	D	P	2	2	27.27	+[a]
	3	*RGS12*	.	.	Missense mutation	SNV	C	T	rs140022951	c.4073C > T	p.P1358L	L	D	P	1	2	22.22	NA
	3	*SETBP1*	+	OG	Missense mutation	SNV	G	A	.	c.2572G > A	p.E858K	L	D	D	1	2	30.77	+[a]
	3	*SMARCA4*	+	TSG	Missense mutation	SNV	G	A	.	c.3067G > A	p.E1023K	N	D	P	1	2	26.67	+[a]
	4	*STMN1*	.	.	Missense mutation	SNV	C	T	.	c.235G > A	p.E79K	M	D	D	2	2	25	+[a]
	3	*ZNRF3*	.	.	Missense mutation	SNV	G	A		c.1361G > A	p.R454H	M	D	D	1	2	21.05	+[a]
2	4	*IWS1*	.	.	Splice site	SNV	T	C	.	c.2048A > G	p.N683S	N	D	B	2	2	21.21	+[b]
	4	*TSC2*	.	.	Nonsense mutation	SNV	C	T	rs45517169	c.1372C > T	p.R458*	.	A	.	2	2	58.33	+[b]

Abbreviations: *A*, disease causing automatic; *B*, benign; *D* (Mutation Taster), disease causing; *D* (Polyphen2 HVAR), probably damaging; *H*, high; *L*, low; *M*, medium; *N*, neutral; *NA*, not available; *OG*, oncogene; *P*, possibly damaging; *TSG*, tumor suppressor gene; *VAF*, variant allele frequency.
Score: Mutect score + Strelka score.
[a] Validation was performed with droplet digital PCR.
[b] Validation was performed with Sanger sequencing.

Table 3. Putative Pathogenic Pathways in TSC-RCC Patients

Case	Gene	Driver	Role	Pathway	Biologic Function	Tumors
1	*CHD8*	–	TSG > OG	Chromatin remodeling	Cell survival; cell proliferation	Hematopoietic malignancy, gastric cancer, colorectal cancer, prostate cancer, breast cancer
	CRISPLD1	–	.	.	.	.
	EPB41L4A	–	.	.	.	Laterally spreading tumor (colorectum), nonmedullary thyroid cancer
	GNA11	+	OG	GPCR pathway	Cell proliferation; cell survival; invasion; apoptosis; differentiation; migration	Melanoma, mesothelioma, endometrial cancer, esophageal cancer, breast cancer, ovarian (mucinous) cancer
	NOTCH3	–	OG > TSG	Notch signaling pathway	Stem-like property; differentiation; cell proliferation; cell motility; invasiveness; metastasis; cell adhesion; epithelial mesenchymal transition; apoptosis; cellular senescence	Breast cancer, T-cell acute lymphoblastic leukemia, B-cell acute lymphoblastic leukemia, ovarian cancer, lung cancer, oral squamous cell carcinoma, pancreatic ductal adenocarcinoma, colorectal carcinoma, skin cancer, melanoma, hepatocellular carcinoma, thyroid cancer, cholangiocarcinoma, renal cell carcinoma, gastric cancer, esophageal cancer, laryngeal cancer, glioblastoma, endometrial cancer, EBV-associated nasopharyngeal cancer, cervical squamous cell carcinoma, chondrosarcoma, Ewing sarcoma family of tumors
	PBRM1	+	TSG	Chromatin remodeling	Cell cycle progression; invasiveness; stemness; differentiation	Clear cell renal cell carcinoma, breast cancer, bladder cancer, cholangiocarcinoma, mesothelioma, gallbladder cancer, prostate cancer, thymic carcinoma, gastric cancer
	PTPRU	–	TSG > OG	Wnt/β-catenin pathway	Cell proliferation, focal adhesion; cell motility; invasiveness	Non–small cell lung carcinoma, small cell lung carcinoma, colon cancer, endometrial cancer, stomach cancer, glioma, melanoma
	RGS12	–	.	GPCR pathway	.	.
	SETBP1	+	OG	PP2A pathway	Cell proliferation; apoptosis; cell survival; cell migration; differentiation	Hematologic malignancy (leukemia, therapy-related myeloid neoplasms, therapy-related acute lymphoblastic leukemia, atypical chronic myeloid leukemia)
	SMARCA4	+	TSG	Chromatin remodeling	Cell cycle progression; invasiveness; stemness; differentiation	Small cell carcinoma of the ovary, hypercalcemic type, non–small cell lung carcinoma, ampullary and pancreatic ductal adenocarcinoma, endometrioid adenocarcinoma, colorectal cancer, rhabdoid tumor, thoracic sarcoma, Wilm tumor, neuroendocrine carcinoma, Burkitt lymphoma, oligodendroglioma, gastric cancer, thymic carcinoma, clear cell renal cell carcinoma, mantle cell lymphoma, cervical cancer, medulloblastoma
	STMN1	–	OG	Microtubule dynamics	Cell cycle progression; invasiveness; metastasis	Gastric cancer, breast cancer, non–small cell lung carcinoma, gallbladder cancer, cutaneous squamous cell carcinoma, oral squamous cell carcinoma, colorectal cancer, osteosarcoma, melanoma, bladder cancer, ovarian cancer, high grade pelvic serous carcinoma, prostate cancer, hepatocellular carcinoma, endometrial cancer, acute myelogenous leukemia, lymphoma, neuroblastoma, mesothelioma, HPV-positive oropharyngeal carcinoma, hypopharyngeal squamous cell carcinoma, nasopharyngeal carcinoma, laryngeal squamous cell carcinoma, small cell lung carcinoma, myelodysplastic syndrome, glioma
	ZNRF3	–	TSG	Wnt/β-catenin pathway	Cell proliferation; apoptosis; cell cycle progression; invasiveness	Colorectal cancer, gastric cancer, lung cancer, papillary thyroid carcinoma, osteosarcoma, adrenocortical carcinoma
2	*IWS1*	–	OG (> TSG)	mRNA processing	Tumor growth; migration; invasiveness	Lung cancer, colon cancer, hepatocellular carcinoma
	TSC2	–	TSG	PI3K/AKT/mTOR pathway	Cell proliferation; cell growth; metabolism; angiogenesis; cell survival; cell mobilization	Lymphangioleiomyomatosis, renal angiomyolipoma, head and neck squamous cell carcinoma, renal cell carcinoma, hamartoma, cortical tuber, subependymal giant cell astrocytoma, angiofibroma

Abbreviations: *OG*, oncogene; *TSG*, tumor suppressor gene.

carcinoma of urinary bladder, hepatocellular carcinoma, and cutaneous malignant melanoma [36, 37]. The *PBRM1* gene is a TSG and is a component of chromatin remodeling pathway and is involved in cell cycle progression, invasiveness, and stemness. *PBRM1* c.49G > A, p.G17R mutation was previously reported in prostate adenocarcinoma [34, 35]. The *PTPRU* gene acts as a TSG and affects Wnt/β-catenin pathway and is involved in cell proliferation, focal adhesion, and invasiveness. *PTPRU* c.1412G > A, p.R471H mutation was not previously reported. The *RGS12* gene is associated with GPCR pathway; however, the pathogenic role on cancer was not established well. *RGS12* c.4073C > T, p.P1358L mutation was in RGS12_usC domain and was not previously reported. The *SETBP1* gene is an OG and affects PP2A pathway and cell proliferation, apoptosis, and cell migration. *SETBP1* c.2572G > A, p.E858K mutation was previously reported in esophageal carcinoma, cutaneous malignant melanoma, esophagus-stomach cancer, and hematopoietic neoplasm [33–35]. The FATHMM prediction was pathogenic [33]. The *SMARCA4* is a TSG and is a component of the chromatin remodeling pathway and is involved in cell cycle progression, invasiveness, and stemness. *SMARCA4* c.3067G > A, p.E1023K mutation was in SNF2_N domain and previously reported in colorectal adenocarcinoma and lung cancer [33–35]. The *STMN1* gene acts as an OG and affects microtubule dynamics and is involved in cell cycle progression, invasiveness, and metastasis. *STMN1* c.235G > A, p.E79K was in Stathmin domain and has not been reported previously. The *ZNRF3* acts as a TSG and affects Wnt/β-catenin pathway and is involved in cell proliferation, apoptosis, and invasiveness. *ZNRF3* c.1361G > A, p.R454H has not been previously reported.

In Case 2, we identified two cancer genes and pathways. The *IWS1* gene acts as an OG and involved in mRNA processing and tumor growth, migration, and invasiveness. *IWS1* c.2048A > G, p.N683S mutation was in Med26 domain and was not previously reported. The *TSC2* gene is thought to be a TSG and is involved in PI3K/AKT/mTOR pathway and affects cell proliferation, metabolism, and cell survival. *TSC2* c.1372C > T, p.R458* was in DUF3384 domain and was previously reported in sporadic pulmonary lymphangioleiomyomatosis [33]. The FATHMM prediction was pathogenic.

It is difficult to determine whether the genetic alterations are pathogenic or not. The “20/20 rule” can be a helpful criterion for identifying driver genes [30]; however, it cannot tell us whether any mutations that are not well documented are pathogenic. One study evaluated mutational signature patterns and reported >200 each TSGs and OGs [31]. However, an aneuploidy pattern without pathogenic features can lead to misinterpretation. The oncogenic *IWS1* gene is predicted as TSG in that study. Mutational features of well-known genes are relatively well documented. For instance, *APC*

mutations within N-terminal 1600 amino acids are pathogenic, and those within C-terminal 1200 amino acids are not. We identified *APC* mutations in Case 2, and the mutation was in C-terminal side. The β-catenin immunohistochemistry revealed no aberrant nuclear expression, consistent with the absence of any pathogenic effect (data not shown). Features of many other driver genes are still unknown. More specific functional studies with base editing and more representative biologic system studies will provide the proper rationale for patient selection and target therapy.

We analyzed mRNA expression on 770 genes. Among the cancer genes from TSC-RCC cases, we evaluated *GNA11*, *NOTCH3*, *PBRM1*, *SETBP1*, *SMARCA4*, and *STMN1* mRNA expression. *NOTCH3* was upregulated and *SETBP1* was downregulated with a two-fold change in Case 1. Among cancers, the *NOTCH3* mRNA expression was upregulated rather than downregulated [33]. The *NOTCH3* mRNA expression with our mutation was 26 percentile in hepatocellular carcinoma and 56 percentile in melanoma [34, 35]. The *SETBP1* mRNA expression was upregulated rather than downregulated in cancers [33]. The *SETBP1* mRNA expression with our mutation was 60 percentile in esophageal carcinoma and 97 percentile in melanoma.

Additionally, in both TSC-RCCs, the mRNA expression of *ALK* and *CRLF2* genes was upregulated, and *CDH1*, *MAP3K1*, *RUNX1*, *SETBP1*, and *TSC1* genes were downregulated. The mRNA expression profile would be useful for the molecular classification rather than individual characterization because mRNA expression can vary in identical cancer types. mRNA expression alone is not sufficient to account for its pathogenic role. Expression can be influenced by genetic mutation, upstream molecules, and interaction with other signaling pathways. Additionally, mRNA expression is not well correlated with protein expression, and upregulation or downregulation does not indicate activation or inactivation. mRNA expression was evaluated in a few genes, and pathogenic pathways cannot be discovered based upon protein-protein interactions. The mRNA expression of previously mentioned genes was evaluated using public data (Supplementary Table 13) [33].

There are some limitations in our study. First, we evaluated just two cases of TSC-RCC due to rarity of this entity. In archival tissue, we could find only two cases of TSC-RCC among 850 RCCs. Second, tumor purity of Case 1 was low, and DNA quality of both cases was relatively low to achieve clear molecular characteristics. Third, we did not perform whole genome sequencing, which could identify large indels, translocations, and fusions. Fourth, we could not perform mRNA sequencing due to poor RNA quality. Alternatively, we analyzed mRNA expression using nanostring. Those limitations should be kept in mind when designing and performing further molecular study.

In summary, we assessed the histopathologic features and genetic alterations in two cases of TSC-RCC. The mTOR activation was assessed by phospho-mTOR immunohistochemistry. WES revealed cancer gene alterations and putative pathogenic pathways that included the chromatin remodeling pathway (*CHD8*, *PBRM1* and *SMARCA4*), GPCR pathway (*GNA11* and *RGS12*), Notch signaling pathway (*NOTCH3*), Wnt/β-catenin pathway (*PTPRU* and *ZNRF3*), PP2A pathway (*SETBP1*), and microtubule dynamics pathway (*STMN1*) in Case 1 and the mRNA processing (*IWS1*) and PI3K/AKT/mTOR pathway (*TSC2*) in Case 2. We evaluated mRNA expression and identified several DEGs, including *ALK*, *CDH1*, *CRLF2*, *MAP3K1*, *RUNX1*, *SETBP1*, and *TSC1*. Also, we suggest additional therapeutic agents. We hope our results will help advance our understanding of the pathogenesis of TSC-RCC, design molecular cancer studies, and translate cancer research into precision medicine.

Funding

This work was supported by grant 03-2015-0230 from the Seoul National University Hospital Research Fund.

Author contributions

J. H. P. and K. C. M. designed the study. Histopathologic review and acquisition of sample were performed by J. H. P., C. L., and K. C. M. The mTOR immunohistochemical study was performed by M. S. C. Primary bioinformatics analysis was performed by J. H. P. Secondary bioinformatics analysis was performed by K. K. and S. C. Validation of cancer genes alterations was performed by H. L. and H. S. L. The manuscript was prepared by J. H. P. Funding acquisition and supervision were performed by K. C. M. All authors participated in the process of finalizing the manuscript. All authors read and approved the final manuscript.

Competing Interests

The authors declare no conflict of interest.

Acknowledgements

We thank Byeong Chul Ghim at Korea Instititue of Toxicology and Byeong-kwon Bae, Jeong-hwa Jang, and Jihye Kim from Bioinformatics Team at DNA Link, Inc., for assistance of primary bioinformatics analysis. We thank Chang-geun Oh and Eun Seo Lim from Next-Generation Sequencing Team at Macrogen, Inc., for assistance of Sanger validation and Circos plot drawing. We thank Sook Lee and Yoo Jung Heo at PhileKorea Technology, Inc., for assistance in mRNA data analysis.

Appendix A. Supplementary data

Supplementary data to this article can be found online at https://doi.org/10.1016/j.tranon.2018.05.010.

References

[1] Rini BI, Rathmell WK, and Godley P (2008). Renal cell carcinoma. *Curr Opin Oncol* **20**, 300–306.

[2] Srigley JR, Delahunt B, Eble JN, Egevad L, Epstein JI, Grignon D, Hes O, Moch H, Montironi R, and Tickoo SK, et al (2013). The International Society of Urological Pathology (ISUP) Vancouver classification of renal neoplasia. *Am J Surg Pathol* **37**, 1469–1489.

[3] Moch H, Amin MB, Argani P, Cheville J, Delahunt B, Martignoni G, Medeiros LJ, Srigley JR, Tan PH, and Tickoo SK (2016). In: Moch H, Humphrey PA, Ulbright TM, Reuter VE, editors. Renal cell tumours: introduction. World Health Organization classification of tumours of the urinary system and male genital organs. 4th edition. Lyon: IARC Press; 2016. p. 14–17.

[4] Edge SB, Byrd DR, Compton CC, Fritz AG, Greene FL, and Trotti A (2009). AJCC Cancer Staging Manual. 7th edition. New York: Springer; 2009 479–489.

[5] Gong J, Gerendash B, Dizman N, Khan A, and Pal SK (2016). Advances in treatment of metastatic renal cell carcinoma. *Curr Opin Urol* **26**, 439–446.

[6] Weinstock M and McDermott D (2015). Targeting PD-1/PD-L1 in the treatment of metastatic renal cell carcinoma. *Ther Adv Urol* **7**, 365–377.

[7] Curtis SA, Cohen JV, and Kluger HM (2016). Evolving immunotherapy approaches for renal cell carcinoma. *Curr Oncol Rep* **18**, 57.

[8] Guo J, Tretiakova MS, Troxell ML, Osunkoya AO, Fadare O, Sangoi AR, Shen SS, Lopez-Beltran A, Mehra R, and Heider A, et al (2014). Tuberous sclerosis-associated renal cell carcinoma: a clinicopathologic study of 57 separate carcinomas in 18 patients. *Am J Surg Pathol* **38**, 1457–1467.

[9] Yang P, Cornejo KM, Sadow PM, Cheng L, Wang M, Xiao Y, Jiang Z, Oliva E, Jozwiak S, and Nussbaum RL, et al (2014). Renal cell carcinoma in tuberous sclerosis complex. *Am J Surg Pathol* **38**, 895–909.

[10] Crino PB, Nathanson KL, and Henske EP (2006). The tuberous sclerosis complex. *N Engl J Med* **355**, 1345–1356.

[11] Northrup H and Krueger DA (2013). International Tuberous Sclerosis Complex Consensus Group. Tuberous sclerosis complex diagnostic criteria update: recommendations of the 2012 International Tuberous Sclerosis Complex Consensus Conference. *Pediatr Neurol* **49**, 243–254.

[12] Cancer Genome Atlas Research Network (2013). Comprehensive molecular characterization of clear cell renal cell carcinoma. *Nature* **499**, 43–49.

[13] Cancer Genome Atlas Research Network (2016). Comprehensive molecular characterization of papillary renal-cell carcinoma. *N Engl J Med* **374**, 135–145.

[14] Davis CF, Ricketts CJ, Wang M, Yang L, Cherniack AD, Shen H, Buhay C, Kang H, Kim SC, and Fahey CC, et al (2014). The somatic genomic landscape of chromophobe renal cell carcinoma. *Cancer Cell* **26**, 319–330.

[15] Manley BJ and Hakimi AA (2016). Molecular profiling of renal cell carcinoma: building a bridge toward clinical impact. *Curr Opin Urol* **26**, 383–387.

[16] Motzer RJ, Escudier B, Oudard S, Hutson TE, Porta C, Bracarda S, Grünwald V, Thompson JA, Figlin RA, and Hollaender N, et al (2008). Efficacy of everolimus in advanced renal cell carcinoma: a double-blind, randomised, placebo-controlled phase III trial. *Lancet* **372**, 449–456.

[17] Collins FS and Varmus H (2015). A new initiative on precision medicine. *N Engl J Med* **372**, 793–795.

[18] Jameson JL and Longo DL (2015). Precision medicine—personalized, problematic, and promising. *N Engl J Med* **372**, 2229–2234.

[19] Delahunt B, Cheville JC, Martignoni G, Humphrey PA, Magi-Galluzzi C, McKenney J, Egevad L, Algaba F, Moch H, and Grignon DJ, et al (2013). The International Society of Urological Pathology (ISUP) grading system for renal cell carcinoma and other prognostic parameters. *Am J Surg Pathol* **37**, 1490–1504.

[20] Andrews S (2010). FastQC. A quality control tool for high throughput sequence data. http://www.bioinformatics.bbsrc.ac.uk/projects/fastqc/; 2010.

[21] Li H and Durbin R (2009). Fast and accurate short read alignment with Burrows-Wheeler transform. *Bioinformatics* **25**, 1754–1760.

[22] McKenna A, Hanna M, Banks E, Sivachenko A, Cibulskis K, Kernytsky A, Garimella K, Altshuler D, Gabriel S, and Daly M, et al (2010). The Genome Analysis Toolkit: a MapReduce framework for analyzing next-generation DNA sequencing data. *Genome Res* **20**, 1297–1303.

[23] Cingolani P, Platts A, Wang le L, Coon M, Nguyen T, Wang L, Land SJ, Lu X, and Ruden DM (2012). A program for annotating and predicting the effects of single nucleotide polymorphisms, SnpEff: SNPs in the genome of Drosophila melanogaster strain w1118; iso-2; iso-3. *Fly (Austin)* **6**, 80–92.

[24] Cibulskis K, Lawrence MS, Carter SL, Sivachenko A, Jaffe D, Sougnez C, Gabriel S, Meyerson M, Lander ES, and Getz G (2013). Sensitive detection of somatic point mutations in impure and heterogeneous cancer samples. *Nat Biotechnol* **31**, 213–219.

[25] Saunders CT, Wong WS, Swamy S, Becq J, Murray LJ, and Cheetham RK (2012). Strelka: accurate somatic small-variant calling from sequenced tumor-normal sample pairs. *Bioinformatics* **28**, 1811–1817.

[26] Ramos AH, Lichtenstein L, Gupta M, Lawrence MS, Pugh TJ, Saksena G, Meyerson M, and Getz G (2015). Oncotator: cancer variant annotation tool. *Hum Mutat* **36**, E2423-2429.

[27] Adzhubei IA, Schmidt S, Peshkin L, Ramensky VE, Gerasimova A, Bork P, Kondrashov AS, and Sunyaev SR (2010). A method and server for predicting damaging missense mutations. *Nat Methods* **7**, 248–249.

[28] Reva B, Antipin Y, and Sander C (2011). Predicting the functional impact of protein mutations: application to cancer genomics. *Nucleic Acids Res* **39**, e118.

[29] Schwarz JM, Cooper DN, Schuelke M, and Seelow D (2014). MutationTaster2: mutation prediction for the deep-sequencing age. *Nat Methods* **11**, 361–362.

[30] Vogelstein B, Papadopoulos N, Velculescu VE, Zhou S, Diaz Jr LA, and Kinzler KW (2013). Cancer genome landscapes. *Science* **339**, 1546–1558.

[31] Davoli T, Xu AW, Mengwasser KE, Sack LM, Yoon JC, Park PJ, and Elledge SJ (2013). Cumulative haploinsufficiency and triplosensitivity drive aneuploidy patterns and shape the cancer genome. *Cell* **155**, 948–962.

[32] Kandoth C, McLellan MD, Vandin F, Ye K, Niu B, Lu C, Xie M, Zhang Q, McMichael JF, and Wyczalkowski MA, et al (2013). Mutational landscape and significance across 12 major cancer types. *Nature* **502**, 333–339.

[33] Forbes SA, Beare D, Gunasekaran P, Leung K, Bindal N, Boutselakis H, Ding M, Bamford S, Cole C, and Ward S, et al (2015). COSMIC: exploring the world's knowledge of somatic mutations in human cancer. *Nucleic Acids Res* **43**, D805–D811.

[34] Cerami E, Gao J, Dogrusoz U, Gross BE, Sumer SO, Aksoy BA, Jacobsen A, Byrne CJ, Heuer ML, and Larsson E, et al (2012). The cBio cancer genomics portal: an open platform for exploring multidimensional cancer genomics data. *Cancer Discov* **2**, 401–404.

[35] Gao J, Aksoy BA, Dogrusoz U, Dresdner G, Gross B, Sumer SO, Sun Y, Jacobsen A, Sinha R, and Larsson E, et al (2013). Integrative analysis of complex cancer genomics and clinical profiles using the cBioPortal. *Sci Signal* **6**pl1.

[36] Kanehisa M and Goto S (2000). KEGG: Kyoto encyclopedia of genes and genomes. *Nucleic Acids Res* **28**, 27–30.

[37] Kanehisa M, Sato Y, Kawashima M, Furumichi M, and Tanabe M (2016). KEGG as a reference resource for gene and protein annotation. *Nucleic Acids Res* **44**, D457–D462.

[38] Robinson JT, Thorvaldsdóttir H, Winckler W, Guttman M, Lander ES, Getz G, and Mesirov JP (2011). Integrative genomics viewer. *Nat Biotechnol* **29**, 24–26.

[39] Thorvaldsdóttir H, Robinson JT, and Mesirov JP (2013). Integrative Genomics Viewer (IGV): high-performance genomics data visualization and exploration. *Brief Bioinform* **14**, 178–192.

[40] Boeva V, Popova T, Bleakley K, Chiche P, Cappo J, Schleiermacher G, Janoueix-Lerosey I, Delattre O, and Barillot E (2012). Control-FREEC: a tool for assessing copy number and allelic content using next-generation sequencing data. *Bioinformatics* **28**, 423–425.

[41] Sathirapongsasuti JF, Lee H, Horst BA, Brunner G, Cochran AJ, Binder S, Quackenbush J, and Nelson SF (2011). Exome sequencing-based copy-number variation and loss of heterozygosity detection: ExomeCNV. *Bioinformatics* **27**, 2648–2654.

[42] Krämer A, Green J, Pollard Jr J, and Tugendreich S (2014). Causal analysis approaches in Ingenuity Pathway Analysis. *Bioinformatics* **30**, 523–530.

[43] Szklarczyk D, Franceschini A, Wyder S, Forslund K, Heller D, Huerta-Cepas J, Simonovic M, Roth A, Santos A, and Tsafou KP, et al (2015). STRING v10: protein-protein interaction networks, integrated over the tree of life. *Nucleic Acids Res* **43**, D447–D452.

[44] Tyburczy ME, Jozwiak S, Malinowska IA, Chekaluk Y, Pugh TJ, Wu CL, Nussbaum RL, Seepo S, Dzik T, and Kotulska K, et al (2015). A shower of second hit events as the cause of multifocal renal cell carcinoma in tuberous sclerosis complex. *Hum Mol Genet* **24**, 1836–1842.

[45] Trpkov K, Hes O, Bonert M, Lopez JI, Bonsib SM, Nesi G, Comperat E, Sibony M, Berney DM, and Martinek P, et al (2016). Eosinophilic, solid, and cystic renal cell carcinoma: clinicopathologic study of 16 unique, sporadic neoplasms occurring in women. *Am J Surg Pathol* **40**, 60–71.

[46] Trpkov K, Abou-Ouf H, Hes O, Lopez JI, Nesi G, Comperat E, Sibony M, Osunkoya AO, Zhou M, and Gokden N, et al (2017). Eosinophilic solid and cystic renal cell carcinoma (ESC RCC): further morphologic and molecular characterization of ESC RCC as a distinct entity. *Am J Surg Pathol* **41**, 1299–1308.

[47] Meric-Bernstam F, Johnson A, Holla V, Bailey AM, Brusco L, Chen K, Routbort M, Patel KP, Zeng J, and Kopetz S, et al (2015). A decision support framework for genomically informed investigational cancer therapy. *J Natl Cancer Inst* **107**.

[48] Martignoni G, Pea M, Rocca PC, and Bonetti F (2003). Renal pathology in the tuberous sclerosis complex. *Pathology* **35**, 505–512.